HHS Public Access

Author manuscript

Dev Biol. Author manuscript; available in PMC 2015 October 23.

Published in final edited form as:

Dev Biol. 2009 January 1; 325(1): 129–137. doi:10.1016/j.ydbio.2008.10.014.

In vivo impact of a 4 bp deletion mutation in the *DLX3* gene on bone development

S.J. Choi[a], **G.D. Roodman**[b], **J.Q. Feng**[c], **I.S. Song**[a], **K. Amin**[a], **P.S. Hart**[d], **J.T. Wright**[e], **N. Haruyama**[f], and **T.C. Hart**[a,*]

[a]Human Craniofacial Genetics Section, Craniofacial and Skeletal Diseases Branch, National Institute of Dental and Craniofacial Research, National Institutes of Health, Bethesda, MD 20854, USA

[b]Department of Medicine, Division of Hematology–Oncology, University of Pittsburgh, Pittsburgh, PA, USA

[c]Biomedical Sciences, Baylor College of Dentistry, Texas A&M Health Science Center, Dallas, TX, USA

[d]Office of the Clinical Director, National Human Genome Research Institute, National Institutes of Health, Bethesda, MD, USA

[e]Department of Pediatric Dentistry, University of North, Chapel Hill, NC, USA

[f]Division of Oral Dysfunction Science, Tohoku University, Graduate School of Dentistry, Sendai, Japan

Abstract

Distal-less 3 (*DLX3*) gene mutations are etiologic for Tricho-Dento-Osseous syndrome. To investigate the *in vivo* impact of mutant *DLX3* on bone development, we established transgenic (TG) mice expressing the c.571_574delGGGG *DLX-3* gene mutation (MT-DLX3) driven by a mouse 2.3 Col1A1 promoter. Microcomputed tomographic analyses demonstrated markedly increased trabecular bone volume and bone mineral density in femora from TG mice. In *ex vivo* experiments, TG mice showed enhanced differentiation of bone marrow stromal cells to osteoblasts and increased expression levels of bone formation markers. However, TG mice did not show enhanced dynamic bone formation rates in *in vivo* fluorochrome double labeling experiments. Osteoclastic differentiation capacities of bone marrow monocytes were reduced in TG mice in the presence of osteoclastogenic factors and the numbers of TRAP(+) osteoclasts on distal metaphyseal trabecular bone surfaces were significantly decreased. TRACP 5b and CTX serum levels were significantly decreased in TG mice, while IFN-γ levels were significantly increased. These data demonstrate that increased levels of IFN-γ decrease osteoclast bone resorption activities, contributing to the enhanced trabecular bone volume and mineral density in these TG mice. These data suggest a novel role for this *DLX-3* mutation in osteoclast differentiation and bone resorption.

*Corresponding author. Fax: +1 301 480 2055. thart@mail.nih.gov (T.C. Hart).

Keywords

Rodent; Transgenic mice; DLX3; Osteoclast; Bone mineralization; Interferon-gamma

Introduction

Tricho-Dento-Osseous (TDO) syndrome is an autosomal dominant disorder clinically characterized by abnormalities in hair, teeth, and bone development. Alterations in osseous tissues are major phenotypic characteristics found in TDO cases due to the *DLX3* c. 571_574delGGGG mutation (NCBI reference sequence; NM_005220), suggesting an association between this mutation and increased thickness and density of bone (Price et al., 1998a; Haldeman et al., 2004). TDO patients with this mutation show increased bone mineral density and thickness in the craniofacial bones, enamel hypoplasia, severe taurodontism, and unique kinky/curly hair (Islam et al., 2005; Wright et al., 1997; Kula et al.,1996). These patients also show increased bone mineral density in long bones (Haldeman et al., 2004; Islam et al., 2005). Bone volume and bone mineral density in the radius and ulna are markedly increased, while bone marrow cavities are markedly reduced, demonstrating enhanced trabeculation of long bones. These data demonstrate that the *DLX3* c.571_574delGGGG mutation alters bone development and homeostasis.

In vitro studies indicate that transduction of the c.571_574delGGGG mutant-*DLX3* (MT-*DLX3*) into C2C12 cells increases osteocalcin gene expression, a bone formation marker, and markedly down-regulates desmin gene expression, a muscle cell differentiation marker (Delmas, 1993; Nakamura et al.,1999; Choi et al., 2008). The 4 bp *DLX3* mutation introduces a frameshift that changes the last C-terminal 97 amino acids (from 191 to 287) creating a novel 119 amino acid C-terminal peptide in the mouse *DLX3* cDNA, just 3′ to the homeobox binding domain. The homeodomain region in both human and mouse *DLX3* genes includes a nuclear localization signal (NLS) from amino acid 130 to 189 (Bryan and Morasso, 2000). The deletion mutation does not alter the structure of the homeobox domain region, the NLS region or the nuclear translocation ability of MT-DLX3 protein. To investigate the *in vivo* impact of MT-DLX3 on bone development, we have established TG mice expressing MT-DLX3 controlled by mouse 2.3 Col1A1 promoter. Here, we report phenotypic bone changes and reduced osteoclastic bone resorption associated with the upregulation of IFN-γ expression in the bone microenvironment in MT-DLX3 transgenic mice.

Materials and methods

Generation of MT-DLX3 TG mice

All experiments were performed under an NIDCR approved animal protocol. A Bam HI restriction site was generated in the mouse 2.3 Col1A1 promoter using the Polymerase Chain Reaction (PCR) with the mouse 2.3 Col1A1 promoter specific primer (5′ TAG GGA TCC CTA GAC CCT AGA CAT GTA GAC 3′; Bam HI site underlined; starting at nt6338755 of GenBank accession number NT_165773.2) and T7 universal primer. The PCR product was subcloned into the Bam HI site and Not I site (multiple cloning site) of the pBS

KS II vector (Stratagene, CA). A mouse MT-DLX3 cDNA with a 4 bp deletion mutation (Choi et al., 2008) was amplified by PCR, using a mouse *DLX3* specific primer (5′ GGG AGA TCT CCA GCA TGA GCG GCT CCT TCG 3′; Bgl II site underlined; starting at 199 bp 5′ of the mouse *DLX3* cDNA (GenBank accession number NM_010055.2)) and the Bgh Rev universal primer. Amplified MT-DLX3 PCR product was double-digested with Bgl II and Xho I, and cloned into the pBS KSII vector containing the 2.3 Col1A1 promoter (Fig. 1A). The identity of the full length MT-DLX3 transgenic construct was confirmed by sequence analysis and the linearized DNA was injected into the pronuclei of fertilized FVB mouse oocytes and implanted into 12 pseudopregnant recipients. Initial genotyping of TG mice was performed by PCR using tail biopsies from pups and primers specific for the 2.3 Col1A1 promoter (Col1A1SS1; 5′ TGC TGT TCT TGG GGG ACT AC 3′) and the MT-DLX3 (AS-4; 5′ GGG GGT CCT TCG TGG AGG GG 3′) starting at nt 1105 (Fig. 1A). Positive founders for the transgene were reconfirmed by genomic southern blot analysis using a ^{32}P dCTP radio-labeled probe. TG mice were bred with wild type mice to generate hemizygotes for the analysis of bone phenotype changes. All mice were fed a soft diet, since defects in tooth mineralization as seen in TDO cases were expected in both male and female TG mice.

Radiographic and microcomputed tomography analysis

Long bones from 6 week- to 12 month-old male TG mice and sex and age matched control littermates were analyzed with a Faxitron MS-20 specimen radiography system for 90 s at 18 kV using X-OMAT Kodak diagnostic film. Femora from the mice were used for three dimensional (3D) microcomputed tomographic (μCT) analyses (Rao et al., 2006). Two dimensional (2D) μCT horizontal slices (thickness 10 μm) of the femur were scanned with a Scanco Viva CT40 (Scanco Medical) and 3D images were reconstituted from 2D scan data, and trabecular bone parameters were measured. Data for a total of 100 slices were obtained on each femur, with sampling 0.1–1.1 mm just below the growth plate in the metaphysis. Parameters analyzed included the ratio of trabecular bone volume per total bone volume, trabecular thickness, trabecular number, trabecular separation, and bone mineral density equivalent mass of hydroxyapatite in a cylindrical area (1.0×1.0×0.5 mm) within the distal metaphyseal area underneath the growth plate-metaphyseal junction as shown in Fig. 2A.

Generation of a specific polyclonal antibody against MT-DLX3 protein and western blot analyses

A MT-DLX3 specific antibody was produced against a polypeptide sequence (C-WPATHRRHQHSGTH, amino acids 204–217) generated by a 4 bp deletion mutation in the mouse *DLX3* gene as described previously (Choi et al., 2008). Three DLX3 antibodies were used: one specific for MT-DLX3 (MT-DLX3 Ab), one specific for WT-DLX3 (C-20, SC-18143, Santa Cruz), and an antibody that recognizes both proteins [6095 antibody] described previously (Choi et al., 2008). To evaluate antibody specificity, western blot analyses were performed using cell lysates from MC3T3E1 cells transfected with the WT-DLX3, MT-DLX3, or empty vector (EV) and stimulated with β-glycerophosphate and ascorbic acid for 5 days. Primary osteoblastic cell lysates from control littermates and TG mice were used to determine the protein expression levels of WT-DLX3, MT-DLX3, runx2, alkaline phosphatase-2 (ALKP-2), β-catenin, and biglycan. WT- and MT-DLX3 (6095 Ab),

WT-DLX3 (C-20 Ab), MT-DLX3 (MT-DLX3 Ab), Runx2 antibody (1:1000, sc-10758, Santa Cruz Biotechnology), ALKP-2 antibody (1:2000, MAB1448, R&D Systems), β-catenin antibody (1:4000, SC-7199, Santa Cruz Biotechnology), and biglycan (1:5000, LF-106, kindly provided by Dr. Larry Fisher, NIDCR) were hybridized to membranes followed by application of Horse Radish Peroxidase (HRP)-conjugated secondary antibody to determine protein expression levels.

Histological and immunohistochemical analyses of long bone

To examine limb trabecular bone structure, standard histological and immunohistochemical analyses were performed. Deparaffinized and rehydrated femora and tibiae sections were incubated with the specific primary antibodies diluted in Antibody Diluent (559148, BD Biosciences) and incubated with HRP conjugated SuperPicture™ Polymer as secondary antibodies (DAB anti-Rabbit; 87-9263 and DAB anti-Goat; 87-9363, Zymed Lab), followed by a DAB coloring reaction. For the detection of WT- and MT-DLX3, slides of long bone sections were incubated with pepsin (Digest-All, 00-3006, Zymed Lab) at 37 °C for 10 min for antigen retrieval and primary antibody was incubated on bone sections as follows: WT-DLX3-specific antibody (1:20) and MT-DLX3-specific antibody (1:400). For immunofluorescence double labeling, rhodamine labeled donkey anti-goat IgG and fluorescein labeled goat anti-rabbit IgG were incubated and epi-fluorescence signals were observed with an inverted fluorescence microscope using TRITC and FITC filters.

Primary mouse bone marrow stromal cell cultures and colony formation assay

Primary bone marrow stromal cells were obtained from 6 week old TG mice and control littermates as previously described (Ehrlich et al., 2005). This cell population was used for the determination of protein expression levels of runx2, ALKP-2, and β-catenin as well as *in vitro* calcium deposition assays. Passage 3 stromal cells (2×10^4) were plated in 48-well plates with α-MEM containing 10% FCS, and 80% confluent cells were treated with osteogenic media (α-MEM with 10% FCS) containing 50 mg/L ascorbic acid, and 10 mM β-glycerophosphate (Franceschi and Lyer, 1992). At day 18, cells were stained for calcium deposition using von Kossa staining and alizarin red S staining. Stained cells were photographed with an inverted microscope, followed by elution of bound alizarin red S with 10% cetylpyridinium chloride (wt/vol) and measurement by spectrophotometry (550 nm) (Stanford et al., 1995). Calcium accumulation was quantified by measurement of acid-soluble calcium with the *o*-cresolphthalein complexone kit (Calcium C-test kit, Waco) (Jono et al., 2000).

Real time PCR analysis

mRNA expression levels for DLX3, runx2, ALKP-2, β-catenin, and biglycan were determined by real time PCR using ABI Taqman Gene Expressionprimers (DLX3; Mm00438428_m1, runx2; Mm03003491_m1, ALKP-2; Mm01187117_m1, β-catenin; Mm01350394_m1, IFN-γ; Mm00801778_m1, GAPDH; Mm99999915_g1) and ABI 7900 HT.

Fluorochrome labeling for the measurement of dynamic bone formation rates

Double fluorochrome *in vivo* labeling using alizarin red S and calcein was performed as described (Sontag, 1980). Seven days after alizarin red S (20 mg/kg) injection, 5 mg/kg of calcein (Sigma–Aldrich) was administrated. Bone specimens were harvested after two days and embedded in methyl-methacrylate. Undecalcified bone sections (10 μm thickness) on glass slides were used to examine epi-fluorescence for the double labeled signal using a fluorescence microscope.

Osteoclast formation assay and osteoclast histomorphometry

Osteoclast formation assays were performed in stromal cell co-culture and stromal cell free culture, using bone marrow monocytic cells and spleen cells from 6 week old male mice (Suda et al., 1997; Kadono et al., 2005). Non-adherent monocytes (10^6/48 well plate) were cultured in α-MEM containing 10% FBS for 6 days in the presence of various concentrations of PTHrP (10 to 100 ng/ml). For osteoclast formation assays in a stromal cell-free system, isolated spleen cells ($5X10^3$/48 well plate) were cultured in α-MEM containing 10% FBS in the presence of 30 ng/ml of recombinant mouse Macrophage Colony Stimulating Factor (rmM-CSF) and varying concentrations (10 to 50 ng/ml) of Receptor Activator of NF kappa B Ligand (RANKL) for 6 days. At day 6, Tartrate-Resistant Acidic Phosphatase (TRAP) staining was performed and the number of TRAP positive multi-nucleated cells (TRAP(+) MNC) were counted using an inverted microscope in a blinded manner. In selected experiments,100 ng/ml of anti-mouse interferon-γ (IFN-γ) antibody (XMG1.2) and 20 pg/ml of IFN-γ were added on culture plates to test the effect of IFN-γ on osteoclast formation.

To identify TRAP(+) osteoclasts on bone sections, specimens were deparaffinized, rehydrated, and stained with TRAP. Osteoclasts were identified as TRAP(+) cells adjacent to trabecular bone. The percent of osteoclast surface per bone surface and the number of osteoclasts per bone surface mm were determined. All measurements were confined to the secondary spongiosa of the femur and restricted to trabecular bone in an area between 0.5 to 1 mm distal from the bone growth plate-metaphyseal junction.

Measurement of serum TRACP 5b, CTX, and interferon-γ levels

To determine osteoclast formation and bone resorption activity *in vivo*, we measured serum Tartrate-Resistant Acid Phosphatase 5b (TRACP 5b) (Alatalo et al., 2000) and carboxy-terminal collagen crosslink (CTX) (Kiviranta et al., 2005) levels using the Mouse TRACP 5b ELISA kits (Immunodiagnostic Systems Inc) and the RatLaps™ ELISA kit (Nordic Bioscience Diagnostics). Serum expression levels of human and mouse IFN-γ were measured using IFN-γ ELISA kit (eBioscience, 88-7914-29 and 88-7916-29). All serum samples were assayed in triplicate in two independent assays. Serum was obtained from TDO affected (n=25) and unaffected (controls; n=15) following informed consent and Human Subjects approval.

Statistical analysis

All statistical analysis was performed by Student's *t*-test (homoscedastic and heteroscedastic) and *p* values less than 0.05 were considered as significantly different.

Results

Generation of MT-DLX3 TG mice

Three lines of MT-DLX3 transgenic (TG) mice were confirmed by genomic southern blot analysis (Fig. 1B). TG mice were bred with wild type mice to produce hemizygotes for phenotype analysis. TG mice appeared normal and fertile. Although the body weights of new born and 14 day-old mice were not different, the body weights of both male and female TG mice were significantly reduced from 6 weeks to 12 months of age (about 30%). The body lengths of both male and female TG mice were similar up to 12 months of age compared to those of control littermates (data not shown). There were no phenotypic differences between male and female TG mice and results for male mice are reported in this manuscript.

Trabecular bone volume and density are significantly increased in MT-DLX3 TG mice

Faxitron radiographic analysis indicated enhanced trabecular bone structure in the femora and tibiae of TG mice compared to those of control littermates from 3 months of age. High-resolution μCT analyses indicated markedly increased trabecular bone volume at the distal metaphyseal area of the femur in TG mice compared to control littermates (Fig. 2A); however cortical bone thickness was not increased in these areas. TG mice have markedly increased trabecular bone volume in the femora from 6 weeks to 12 months of age (Fig. 2B). Quantification of trabecular bone morphometry in the yellow cylindrical volume underneath the femur growth plate in three sex and age matched specimens from 3 to 5 month old mice revealed that the trabecular bone volume per tissue volume was significantly higher in TG mice than control mice (Fig. 2Ca). While the average thickness of the trabeculae (Fig. 2Cb) was not significantly different, the average number of trabeculae (Fig. 2Cc) was significantly increased in TG mice and the average space between trabeculae (Fig. 2Cd) was significantly reduced. Importantly, the bone mineral density equivalent mass of hydroxyapatite in these yellow cylindrical areas was significantly increased in TG mice (Fig. 2Ce).

Expression pattern of WT-DLX3 and MT-DLX3 protein in limb of MT-DLX3 TG mice

The specificities of the three DLX3 antibodies were demonstrated in western blot analyses of cell lysates from differentiated MC3T3E1 cells, transfected with either empty vector, WT-DLX3 and MT-DLX3. DLX3 6095 antibody detected both WT-DLX3 and MT-DLX3 proteins, WT-DLX3 specific C-terminal antibody (C-20, SC-18143) detected only WT-DLX3 protein and MT-DLX3 specific antibody detected only MT-DLX3 protein (Fig. 3A). Primary osteoblasts from TG mice express ~2.3 times the level of total DLX3 mRNA (WT- plus MT-DLX3 mRNA) compared to control littermates (WT-DLX3 only) (Fig. 3B). Expression of WT- and MT-DLX3 proteins in primary osteoblasts from TG mice was assessed by western blot analyses. Control littermates expressed only WT-DLX3 and TG

mice expressed both WT- and MT-DLX3 proteins (Fig. 3C). As previously reported (Choi et al., 2008), this deletion mutation introduces frameshift producing a longer open reading frame frameshift and generation of a 35 kDa MT-DLX3. Quantification of DLX3 protein expression levels in primary osteoblasts indicated that TG mice expressed endogenous WT-DLX3 protein at similar levels with those of control littermates and expressed MT-DLX3 protein at a slightly higher level (1.2 fold) compared to endogenous WT-DLX3 (Fig. 3C). Immunohistochemical staining demonstrated both WT- and MT-DLX3 proteins were expressed in the nuclei of osteoblasts (indicated with arrow head) and osteocytes (indicated with arrow) in bone sections from TG mice, while only WT-DXL3 protein was detected in the nuclei of osteoblasts and osteocytes of bone sections from control littermates (Fig. 3D). Immunofluorescence double labeling demonstrated that both WT-DLX3 protein (red) and MT-DLX3 protein (green) were expressed in the nuclei of cultured primary osteoblasts from TG mice (Fig. 3E). MT-DLX3 protein expression was not detected in osteoclast precursors or in mature osteoclasts by immunohistochemical methods in bone sections as well as cultured osteoclasts from bone marrow and spleen cells of TG mice (data not shown).

Effects of MT-DLX3 on osteoblastic bone formation in vitro and in vivo

To examine the osteogenic differentiation efficiency of bone marrow stromal cells to osteoblasts, passage three primary bone marrow stromal cells from TG mice and control littermates were differentiated into osteoblasts by treatment with osteogenic media. As shown in Fig. 4A, calcium deposition was markedly increased in primary stromal cells cultured for 18 days from TG mice as indicated by alizarin red S and von Kossa staining. Quantification of the alizarin red S bound on the culture plates and mineralized nodules formed on culture plates revealed that primary bone marrow stromal cells from TG mice have increased calcium deposition capacities during osteoblastic differentiation. We then performed real time PCR and western blot analysis to determine whether MT-DLX3 increased the expression of osteoblast differentiation markers in the passage three primary osteoblasts stimulated with osteogenic media for 10 days. As shown in Fig. 4B, mRNA expression levels of runx2, alkaline phosphatase-2, and β-catenin were significantly increased in primary osteoblasts from MT-DLX3 TG mice. Western blot analyses also demonstrated that the expression levels of bone formation markers, runx2, ALKP-2, and β-catenin, were upregulated in primary osteoblast from TG mice (Fig. 4C).

To examine the impact of MT-DLX3 on the dynamic *in vivo* bone formation rate, we performed alizarin red S and calcein double labeling studies on 6 week old male mice. As indicated by white arrows in Fig. 4D lower panels, the double lines labeled by alizarin red S and calcein on the non-decalcified bone sections were not different between TG mice and control littermates. Histomorphometric analysis revealed that static bone formation parameters were not significantly different between TG and control littermates. Furthermore, the number of single and double labeled surfaces and the distance between the two double-labeled surfaces for the calculation of the mineral apposition rate (MAR) were also not significantly different. Consequently, while osteoblast differentiation and nodule formation rates in an *ex vivo* assay, were increased in TG bone marrow stromal cells, *in vivo* bone formation rates were not increased in TG mice.

Effects of MT-DLX3 on osteoclastic bone resorption

Since we did not see enhanced bone formation in TG mice *in vivo*, we investigated the effects of MT-DLX3 on osteoclast differentiation and bone resorption using mouse bone marrow (containing stromal cells) and spleen cells (stromal cell free). The number of TRAP(+) osteoclast-like MNC increased in a dose-dependent manner in the cultured bone marrow cells from control littermates in the presence of 50–100 ng/ml of PTHrP (Fig. 5A). In contrast, TRAP(+) osteoclast-like MNC formation was not increased in the cultured bone marrow cells from the TG mice. We performed osteoclast-like MNC formation assays using a stromal cell free assay system to test whether the defect in osteoclastogenesis in TG mice was due to abnormalities of stromal cells. As shown in Fig. 5A right panel, the numbers of TRAP(+) osteoclast-like MNC were dose dependently increased in the cultured spleen cells from control littermates in the presence of 30 ng/ml of rmM-CSF and varying concentrations of RANKL. However, the number of TRAP(+) osteoclast-like MNC was not increased in cultured spleen cells from TG mice by RANKL and M-CSF treatment.

TRAP staining was performed on the bone sections to identify osteoclasts. The number of TRAP(+) osteoclasts in the distal metaphyseal area under the bone growth plate cartilage of TG mice was markedly reduced compared to those of control littermates (Figs. 5Ba, 5Bc). To quantify TRAP(+) osteoclasts, histomorphometric analysis was performed. TRAP(+) osteoclasts per bone surface in the distal metaphyseal area of TG mice were significantly reduced (Fig. 5C left panel). Similarly, the numbers of osteoclasts per mm bone surface were significantly decreased in MT-DLX3 TG mice (Fig. 5C right panel). We then examined the serum levels of TRACP 5b associated with *in vivo* osteoclast formation and CTX representing the *in vivo* osteoclastic bone resorption activity. The serum expression levels of TRACP 5b and CTX were significantly reduced in TG mice (Fig. 5D).

Expression levels of IFN-γ in serum and neutralizing effect of anti-mouse IFN-γ antibody on osteoclast formation

To identify factor(s) responsible for the defect in osteoclastogenesis, gene expression profiling using the RT^2 PCR profiler array (PAMM-011,-018,-024,-025,-053,-064, Superarray Bioscience, MD) and cDNA from bone marrow and spleen was performed. IFN-γ mRNA expression levels were consistently up-regulated in TG mice. Real time PCR results demonstrated that IFN-γ mRNA expression levels were markedly increased in bone marrow cells (3.35±1.26 fold) and spleen cells (2.36±0.86 fold) from TG mice compared to those of control littermates. We then measured serum expression level of mouse IFN-γ. As shown in Fig. 6A, serum IFN-γ expression levels were significantly increased in TG mice (about 5 fold). Furthermore human IFN-γ expression levels were also significantly increased in serum from patients with TDO syndrome compared to unaffected control individuals (7.3±6.1 versus 16.4±11 pg/ml) (Fig. 6B). To test whether IFN-γ is responsible for decreased osteoclast formation in TG mice, we performed osteoclast formation assays. As shown in Fig. 6C, the number of osteoclast stimulated with 30 ng/ml of RANKL was decreased in bone marrow culture from control littermates in the presence of 20 pg/ml of IFN-γ, and 100 ng/ml of anti mouse IFN-γ antibody reversed the inhibitory activity of IFN-γ. Osteoclast formation in bone marrow cells from TG mice was decreased compared to

those of control littermate in the presence of 30 ng/ml of RANKL while treatment with 100 ng/ml of anti mouse IFN-γ antibody significantly increased osteoclast numbers.

Discussion

The *DLX3* c.571_574delGGGG is the most common mutation that causes TDO (Price et al., 1998a; Haldeman et al., 2004; Islam et al., 2005; Price et al., 1998b). While affected individuals show increased thickness and density of craniofacial and appendicular bones, it is unknown if this arises from increased bone formation, decreased bone resorption or a combination of both. To investigate the *in vivo* impact of this 4 bp *DLX3* deletion mutation on bone development, we generated MT-DLX3 TG mice using the 2.3 Col1A1 promoter.

Since the 2.3 Col1A1 promoter is bone and tooth specific, we evaluated DLX3 mRNA and protein expression levels using primary osteoblasts from TG hemizygous mice. Total DLX3 mRNA expression in primary osteoblasts of TG mice was 2.3 fold greater than WT-DLX3 expression in WT-mice, indicating an expression ratio of ~1.3:1 for MT-DLX3: WT-DXL3 in the TG mice. RT-PCR demonstrated MT-DLX3 levels were similar to those of WT-DLX3 in TG mice (data not shown). Furthermore, expression levels of MT-DLX3 protein in cultured primary osteoblasts were similar to WT-DLX3 protein in both TG and control littermates. Consistent with our observation, multiple reports (Kanatani et al., 2006; Gori et al., 2006; Schmidt et al., 2005; Jiang et al., 2006) have demonstrated that the 2.3 Col1A1 promoter expresses target proteins in a tissue specific pattern rather than gross overexpression specifically in hemizygous mice.

Radiographic and microcomputed tomographic (μCT) analyses of long bones demonstrated dramatically enhanced trabecular bone in the distal metaphyseal area of femurs in TG mice from 6 weeks of age, consistent with clinical observations in humans with TDO (Price et al., 1998a; Haldeman et al., 2004; Islam et al., 2005; Wright et al., 1997; Kula et al., 1996). While tooth eruption was not altered, TG mice manifested an abnormal tooth phenotype, characterized by large pulp chambers and defects in dentin mineralization (data not shown), clinical findings also seen in TDO patients. We speculate that the reduced body weight seen in both male and female TG mice may be a consequence of eating stress.

Primary bone marrow stromal cells isolated from long bones of TG mice cultured with osteogenic media displayed enhanced ALKP-2 activity and calcium deposition. Additionally, mRNA and protein expression of runx2, ALKP-2, and β-catenin, which are major osteoblastic differentiation and bone formation markers (Garimella et al., 2004; Rodan and Noda, 1991), were up-regulated in primary bone marrow stromal cells from TG mice. While, TG mice did not show an enhanced rate of dynamic bone formation by *in vivo* fluorochrome double labeling experiments, decreased osteoclast formation and decreased osteoclastic bone resorption activity was observed. TG mice demonstrated decreased numbers of osteoclasts on distal metaphyseal trabecular bone surfaces, and significantly reduced serum levels of TRACP 5b and CTX. We did not see differences in the expression levels of RANKL and osteoprotegerin in western blot and real time PCR analyses using primary osteoblasts from TG mice and control littermates (data not shown). These data suggest that the defect in osteoclast formation and bone resorption seen in TG mice might

not be due to abnormalities in stromal cells. Interestingly, TRAP(+) osteoclasts were markedly reduced in the distal metaphyseal area but not in the proximal metaphyseal area. MT-DLX3 protein was not expressed in osteoclasts from TG mice. These data suggest that highly localized bone microenvironmental factors produced by bone marrow cells may be responsible for the reduced osteoclastic bone resorption in TG mice. Recent reports demonstrated that T lymphocytes and their products have been recognized as key regulators of osteoclast formation (Weitzmann and Pacifici, 2007; Takayanagi et al., 2000). Therefore, we performed gene expression profiling using the RT^2 PCR profiler array (Superarray Bioscience, MD) with bone marrow and spleen cDNA. IFN-γ mRNA expression levels were consistently up-regulated in TG mice. IFN-γ can act as a potent osteoclastogenesis inhibitor by interfering in the RANK–RANKL signaling pathway. IFN-γ induces rapid degradation of the RANK adaptor protein, TRAF6 (tumor necrosis factor receptor associated factor 6) (Takayanagi et al., 2002). We found that mRNA expression levels of IFN-γ were significantly increased in bone marrow cells (3.35±1.26 fold) and spleen cells (2.36±0.86 fold) from TG mice compared to control littermates. Serum levels of IFN-γ were also elevated in TG mice (about 5 fold) and in serum specimens from patients with TDO syndrome compared to unaffected family members (greater than 2 fold increase). Furthermore, 20 pg/ml of IFN-γ significantly decreased the number of osteoclasts formed in bone marrow cell culture from control littermates stimulated with 30 ng/ml of RANKL. Addition of anti mouse IFN-γ antibody (100 ng/ml) reversed the inhibitory effects of IFN-γ on osteoclast formation. Interestingly, treatment of anti mouse IFN-γ antibody significantly increased the number of osteoclasts in bone marrow cell cultures from TG mice. These data suggest that elevated IFN-γ expression appears to be responsible for the defective osteoclast formation and bone resorption in TG mice. Consistent with our results, Kamolmatyakul et al. reported that 0.2 IU/ml (approximately 40 pg/ml) of IFN-γ markedly and significantly decreased osteoclast formation *in vitro* (Kamolmatyakul et al., 2001). Takahashi et al. also reported that less than 1 IU/ml (approximately 200 pg/ml) of IFN-γ dramatically decreased human osteoclast formation (Takahashi et al. 1986).

Up-regulated IFN-γ expression levels in TG mice may also explain the apparent discrepancy between *in vivo* and *ex vivo* results for the effects of MT-DLX3 on osteoblast formation and osteoblastic bone formation. Our previous report demonstrated that transduction of MT-DLX3 into C2C12 cells increased osteoblastic differentiation and calcium deposition *in vitro* (Choi et al., 2008). Furthermore, our *ex vivo* study demonstrated that the primary stromal cells from TG mice showed enhanced osteoblast differentiation and calcium deposition. However, TG mice did not show enhanced *in vivo* bone formation. *Ex vivo* assays for osteoblastic bone formation using passage three primary stromal cells from mice did not contain immune cells such as T lymphocytes that express IFN-γ. However, the bone microenvironment contains cells that express IFN-γ, which is known to act as an inhibitory factor for osteoblastic bone formation. Although, *in vitro* and *ex vivo* data showed enhanced osteoblast differentiation and nodule formation, systemic modulating factors such as IFN-γ might attenuate or compensate the effects of bone formation *in vivo*. In our TG mice, increased expression levels of IFN-γ inhibit osteoblastic bone formation and decrease osteoclastic bone resorption *in vivo*. Smith et al. reported that 10^{-10} M of IFN-γ significantly decreased the expression of collagenase digestible protein (CDP) and non-collagenase

digestible protein (NDP) in fetal rat bone cultures (Smith et al., 1987). Amento et al. also reported that 0.1 IU of IFN-γ markedly induced class II antigen expression on adherent synovial cells (Amento et al., 1985). These data demonstrated that IFN-γ suppressed osteoblast differentiation as well as osteoblastic bone formation by inhibiting bone collagen synthesis. Interestingly, we could not detect IFN-γ expression in passage three stromal cells or differentiated osteoblasts from TG mice. We speculate that MT-DLX3 expression by osteogenic cells must be causing changes in cytokine/growth factor expression that induce IFN-γ production by other cells, possibly T lymphocytes, via unknown mechanisms. We also cannot exclude the possibilities that other locally produced autocrine/paracrine and systemic endocrine factors, such as osteogenic growth peptide (OGP) (Bab et al., 1992), parathyroid hormone related peptide (PTHrP) (Karaplis and Deckelbaum, 1998), and insulin-like growth factors (IGF) (Bab and Einhorn, 1993), which have critical roles in osteoblastic bone formation, may have additional effects on osteoblastic bone formation in TG mice.

The molecular pathways controlled by MT-DLX3 in osteoblast differentiation are unknown. We found that the mRNA and protein expression levels of runx2 were enhanced in primary osteoprogenitors from TG mice (Figs. 4B, 4C). In contrast, Duverger et al. (2008) recently reported that MT-DLX3 showed a dominant negative effect on WT-DLX3 transcriptional activity in a transiently transfected cell model system, even though co-expression of WT- and MT-DLX3 proteins forms a complex with the homeobox binding domain element. This condition appears to be a dramatic overexpression of MT-DLX3 that might saturate MT-DLX3 protein and dysregulate DLX3 transcription machinery associated with other co-factors and not reflect the biologic conditions associated with TDO syndrome. Hassan et al., (2004, 2008) reported that DLX3 is ubiquitously expressed in many cell types. It's functional cell specificities are controlled by the selective association with HOXA10, MSX2, RUNX2, and DLX5 homeodomain transcription factors resulting in the repression, activation and attenuation of bone specific genes transcription. These data demonstrate that MT-DLX3 with endogenous WT-DLX3 could bind the homeobox domain binding motif of osteogenic factor genes and positively or negatively regulate runx2 expression as well as other osteogenic genes via unknown pathway depending on the association of co-factors.

Taken together, these findings indicate that decreased osteoclastic bone resorption activity due to the increased IFN-γ expression by immune cells increased trabecular bone volume and density in TG mice. These results suggest a gain of function mutation induced change in hematopoietic cells, either those that form osteoclasts or in those that regulate osteoclast formation. While we do not know how MT-DLX3 influences IFN-γ expression in immune cells, skeletal homeostasis is greatly influenced by components of the immune system (Rho et al., 2004). Our findings are consistent with opposing intrinsic and extrinsic effects. Although, *in vitro* and *ex vivo* data showed enhanced osteoblast differentiation and nodule formation, systemic modulating factors such as IFN-γ may attenuate or compensate the dramatic effects of bone formation *in vivo*. Immune cell types with selective cytokine production affect bone cell differentiation and bone homeostasis. Cells that regulate bone turnover share a common precursor with inflammatory immune cells and may restrict themselves anatomically, in part, by utilizing a signaling network analogous to lymphocyte

co-stimulation (Walsh et al., 2006). Further study is needed to understand the role of this *DLX3* deletion mutation in immune cell responses including IFN-γ production.

Acknowledgments

We thank Dr. Pamela Robey and Dr. Marian Young of the National Institute of Dental and Craniofacial Research, NIH, for their critique of this manuscript. This work was supported in part by the Intramural Program of the National Institute of Dental and Craniofacial Research, National Institutes of Health, Bethesda, MD.

References

Alatalo SL, Halleen JM, Hentunen TA, Mönkkönen J, Väänänen HK. Rapid screening method for osteoclast differentiation *in vitro* that measures tartrate-resistant acid phosphatase 5b activity secreted into the culture medium. Clin Chem. 2000; 46:1751–1754. [PubMed: 11067809]

Amento EP, Bhan AK, McCullagh KG, Krane SM. Influences of gamma interferon on synovial fibroblast-like cells. Ia induction and inhibition of collagen synthesis. J Clin Invest. 1985; 76:837–848. [PubMed: 2993365]

Bab IA, Einhorn TA. Regulatory role of osteogenic growth polypeptides in bone formation and hemopoiesis. Crit Rev Eukaryot Gene Expr. 1993; 3:31–46. [PubMed: 8439709]

Bab I, Gazit D, Chorev M, Muhlrad A, Shteyer A, Greenberg Z, Namdar M, Kahn A. Histone H4-related osteogenic growth peptide (OGP): a novel circulating stimulator of osteoblastic activity. EMBO. 1992; 11:1867–1873.

Bryan JT, Morasso MI. The DLX3 protein harbors basic residues required for nuclear localization, transcriptional activity and binding to MSX1. J Cell Sci. 2000; 113:4013–4023. [PubMed: 11058088]

Choi SJ, Song IS, Ryu OH, Choi SW, Hart PS, Wu WW, Shen RF, Hart TC. A 4 bp deletion mutation in *DLX3* enhances osteoblastic differentiation and bone formation *in vitro*. Bone. 2008; 42:162–171. [PubMed: 17950683]

Delmas PD. Biochemical markers of bone turnover. I: Theoretical considerations and clinical use in osteoporosis. Am J Med. 1993; 95:11S–16S. [PubMed: 8256787]

Duverger O, Lee D, Hassan MQ, Chen SX, Jaisser F, Lian JB, Morasso MI. Molecular consequences of a frameshifted *DLX3* mutant leading to Tricho-Dento-Osseous syndrome. J Biol Chem. 2008; 283:20198–20208. [PubMed: 18492670]

Ehrlich LA, Chung HY, Ghobrial I, Choi SJ, Morandi F, Colla S, Rizzoli V, Roodman GD, Giuliani N. IL-3 is a potential inhibitor of osteoblast differentiation in multiple myeloma. Blood. 2005; 106:1407–1414. [PubMed: 15878977]

Franceschi RT, Lyer BS. Relationship between collagen synthesis and expression of the osteoblast phenotype in MC3T3-E1 cells. J Bone Miner Res. 1992; 7:235–246. [PubMed: 1373931]

Garimella R, Bi X, Camacho N, Sipe JB, Anderson HC. Primary culture of rat growth plate chondrocytes: an *in vitro* model of growth plate histotype, matrix vesicle biogenesis and mineralization. Bone. 2004; 34:961–970. [PubMed: 15193542]

Gori F, Friedman LG, Demay MB. Wdr5, a WD-40 protein, regulates osteoblast differentiation during embryonic bone development. Dev Biol. 2006; 295:498–506. [PubMed: 16730692]

Haldeman RJ, Cooper LF, Hart TC, Phillips C, Boyd C, Lester GE, Wright JT. Increased bone density associated with *DLX3* mutation in the Tricho-Dento-Osseous syndrome. Bone. 2004; 35:988–997. [PubMed: 15454107]

Hassan MQ, Javed A, Morasso MI, Karlin J, Montecino M, van Wijnen AJ, Stein GS, Stein JL, Lian JB. DLX3 transcriptional regulation of osteoblast differentiation: temporal recruitment of MSX2, DLX3, and DLX5 homeodomain proteins to chromatin of the osteocalcin gene. Mol Cell Biol. 2004; 24:9248–9261. [PubMed: 15456894]

Hassan MQ, Saini S, Gordon JAR, van Wijnen AJ, Montecino M, Stein JL, Stein GS, Lian JB. Molecular switches involving homeodomain proteins, HOXA10 and RUNX2 regulate osteoblastogenesis. Cells Tissues Organs. 2008 Aug.:14. Epub ahead of print.

Islam M, Lurie AG, Reichenberger E. Clinical features of Tricho-Dento-Osseous syndrome and presentation of three new cases: an addition to clinical heterogeneity. Oral Surg Oral Med Oral Pathol Oral Radiol Endod. 2005; 100:736–742. [PubMed: 16301156]

Jiang J, Lichtler AC, Gronowicz GA, Adams DJ, Clark SH, Rosen CJ, Kream BE. Transgenic mice with osteoblast-targeted insulin-like growth factor-I show increased bone remodeling. Bone. 2006; 39:494–504. [PubMed: 16644298]

Jono S, Peinado C, Giachelli CM. Phosphorylation of osteopontin is required for inhibition of vascular smooth muscle cell calcification. J Biol Chem. 2000; 275:20197–20203. [PubMed: 10766759]

Kadono Y, Okada F, Perchonock C, Jang HD, Lee SY, Kim N, Choi Y. Strength of TRAF6 signaling determines osteoclastogenesis. EMBO. 2005; 6:171–176.

Kamolmatyakul S, Chen W, Li YP. Interferon-gamma down-regulates gene expression of cathepsin K in osteoclasts and inhibits osteoclast formation. J Dent Res. 2001; 80:351–355. [PubMed: 11269728]

Kanatani N, Fujita T, Fukuyama R, Liu W, Yoshida CA, Moriishi T, Yamana K, Miyazaki T, Toyosawa S, Komori T. Cbfbeta regulates Runx2 function isoform-dependently in postnatal bone development. Dev Biol. 2006; 296:48–61. [PubMed: 16797526]

Karaplis AC, Deckelbaum RA. Role of PTHrP and PTH-1 receptor in endochondral bone development. Front Biosci. 1998; 3:795–803.

Kiviranta R, Morko J, Alatalo SL, NicAmhlaoibh R, Risteli J, Laitala-Leinonen T, Vuorio E. Impaired bone resorption in cathepsin K-deficient mice is partially compensated for by enhanced osteoclastogenesis and increased expression of other proteases via an increased RANKL/OPG ratio. Bone. 2005; 36:159–172. [PubMed: 15664014]

Kula K, Hall K, Hart T, Wright JT. Craniofacial morphology of the Tricho-Dento-Osseous syndrome. Clin Genet. 1996; 50:446–454. [PubMed: 9147871]

Nakamura T, Takeuchi K, Muraoka S, Muneoka K, Takigawa M. A neurally enriched coronin-like protein, ClipinC, is a novel candidate for an actin cytoskeleton-cortical membrane-linking protein. J Biol Chem. 1999; 274:13322–13327. [PubMed: 10224093]

Price JA, Bowden DW, Wright JT, Pettenati MJ, Hart TC. Identification of a mutation in *DLX3* associated with Tricho-Dento-Osseous (TDO) syndrome. Hum Mol Genet. 1998a; 7:563–569. [PubMed: 9467018]

Price JA, Wright JT, Kula K, Bowden DW, Hart TC. A common *DLX3* gene mutation is responsible for Tricho-Dento-Osseous syndrome in Virginia and North Carolina families. J Med Genet. 1998b; 35:825–828. [PubMed: 9783705]

Rao H, Lu G, Kajiya H, Garcia-Palacios V, Kurihara N, Anderson J, Patrene K, Sheppard D, Blair HC, Windle JJ, Choi SJ, Roodman GD. $\alpha_9\beta_1$: a novel osteoclast integrin that regulates osteoclast formation and function. J Bone Miner Res. 2006; 21:1657–1665. [PubMed: 16995821]

Rho J, Takami M, Choi Y. Osteoimmunology: interactions of the immune and skeletal systems. Mol Cells. 2004; 17:1–9. [PubMed: 15055519]

Rodan GA, Noda M. Gene expression in osteoblastic cells. Crit Rev Eukaryot Gene Exp. 1991; 1:85–98.

Schmidt K, Schinke T, Haberland M, Priemel M, Schilling AF, Mueldner C, Rueger JM, Sock E, Wegner M, Amling M. The high mobility group transcription factor Sox8 is a negative regulator of osteoblast differentiation. J Cell Biol. 2005; 168:899–910. [PubMed: 15753123]

Smith DD, Gowen M, Mundy GR. Effects of interferon-gamma and other cytokines on collagen synthesis in fetal rat bone cultures. Endocrinology. 1987; 120:2494–2499. [PubMed: 3106020]

Sontag W. An automatic microspectrophotometric scanning method for the measurement of bone formation rates *in vivo*. Calcif Tissue Int. 1980; 32:63–68. [PubMed: 6159059]

Stanford CM, Jacobson PA, Eanes ED, Lembke LA, Midura RJ. Rapidly forming apatitic mineral in an osteoblastic cell line (UMR 106-01 BSP). J Biol Chem. 1995; 270:9420–9428. [PubMed: 7721867]

Suda T, Jimi E, Nakamura I, Takahashi N. Role of 1α,25-dihydroxyvitamin D3 in osteoclast differentiation and function. Methods Enzymol. 1997; 282:223–235. [PubMed: 9330291]

Takahashi N, Mundy GR, Roodman GD. Recombinant human interferon-gamma inhibits formation of human osteoclast-like cells. J Immunol. 1986; 137:3544–3549. [PubMed: 3097126]

Takayanagi H, Ogasawara K, Hida S, Chiba T, Murata S, Sato K, Takaoka A, Yokochi T, Oda H, Tanaka K, Nakamura K, Taniguchi T. T-cell-mediated regulation of osteoclastogenesis by signaling cross-talk between RANKL and IFN-γ. Nature. 2000; 408:600–605. [PubMed: 11117749]

Takayanagi H, Kim S, Taniguchi T. Signaling crosstalk between RANKL and interferons in osteoclast differentiation. Arthritis Res. 2002; 4:S227–S232. [PubMed: 12110142]

Walsh MC, Kim N, Kadono Y, Rho J, Lee SY, Lorenzo J, Choi Y. Osteoimmunology: interplay between the immune system and bone metabolism. Annu Rev Immunol. 2006; 24:33–63. [PubMed: 16551243]

Weitzmann MN, Pacifici R. T cells: unexpected players in the bone loss induced by estrogen deficiency and in basal bone homeostasis. Ann NY Acad Sci. 2007; 1116:360–375. [PubMed: 18083938]

Wright JT, Kula K, Hall K, Simmons JH, Hart TC. Analysis of the Tricho-Dento-Osseous syndrome genotype and phenotype. Am J Med Genet. 1997; 72:197–204. [PubMed: 9382143]

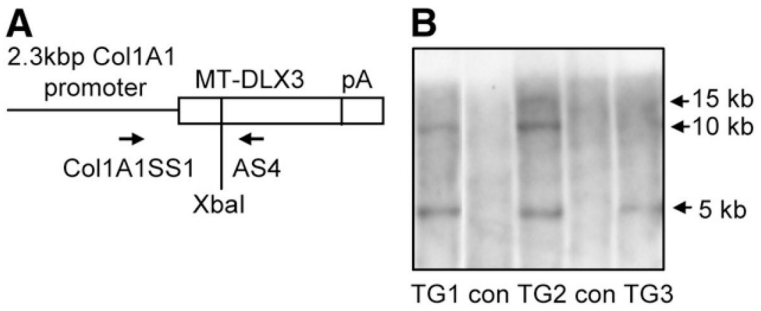

Fig. 1.

(A) Schematic diagram of Col1A1 MT-DLX3 TG construct (5 kb) containing mouse 2.3 kb type I collagen promoter, 2.7 kb mouse MT-DLX3 cDNA, and Bgh poly A tail (pA). Col1A1SS1 and AS4 primers were used for the PCR genotyping. (B) XbaI digested chromosomal DNA from tail biopsies was used for genomic southern blot analyses. Three TG lines (TG1, TG2, and TG3) were identified (Con: non transgenic control). The 5 kb transgene bands were detected in TG1, TG2 and TG3.

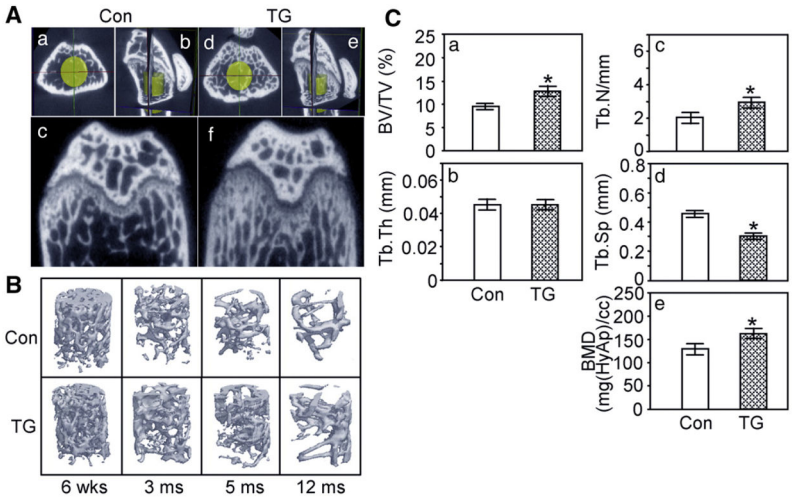

Fig. 2.

Microcomputed tomography of femora from male TG and male control mice. (A) Two dimensional views of 3 month old male mice (a,b,c, control littermate; d,e,f, TG mouse; a, d, axial view; c,f, coronal view; b,e, cubic view; yellow cylinder represents an isotropic voxel area for the evaluation of the trabecular bone morphometric parameters). (B) Three-dimensional structure of trabecular bone from 6 week- to 12 month-old male mice. (C) Quantification of trabecular bone morphometric parameters. (BV/TV, bone volume per total tissue volume (a); Tb.Th, trabecular bone thickness (b); Tb.N, trabecular bone number (c); Tb.Sp, trabecular bone space (d); BMD, bone mineral density equivalent mass of hydroxyapatite mg [HyAp/CC] (e); (*p*: * <0.05, data represent mean±SEM).

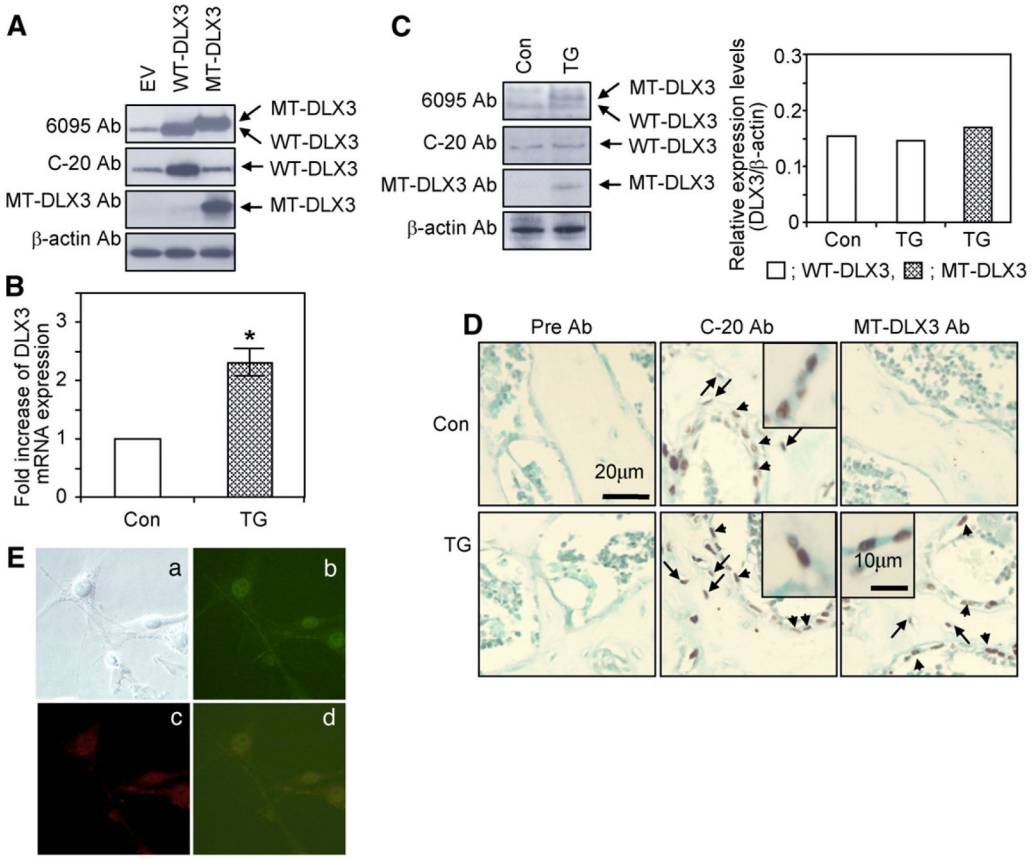

Fig. 3.

Expression of WT- and MT-DLX3. (A) Western blot analyses performed using the 6095 antibody that detects both WT- and MT-DLX3 proteins, C-20 antibody that detects WT-DLX3 protein, and a MT-DLX3 specific antibody in MC3T3E1 cells transfected with empty vector (EV), WT-DLX3, and MT-DLX3. (B) Real time PCR analysis demonstrating DLX3 mRNA expression in primary osteoblasts from Transgenic (TG) compared to control (Con) littermates. Fold increase represents the ratio of 2^-(Ct(Target)-Ct(GAPDH))$^{(TG)}$/2^-(Ct(Target)-Ct(GAPDH))$^{(Con)}$ (p: * <0.05, data represent mean±SEM). (C) Primary osteoblasts from TG mice expressing both WT- and MT-DLX3 proteins and cells from control littermates expressing only WT-DLX3 protein (left panel). Quantification of WT- and MT-DLX3 proteins in primary osteoblasts (open bar; WT-DLX3, hatched bar; MT-DLX3) (right panel). (D) Immunohistochemical detection of WT- and MT-DLX3 proteins in bone sections from 6 week old male MT-DLX3 TG mice. WT-DLX3 protein but not MT-DLX3 protein was detected in of osteoblasts as indicated by arrowheads and osteocytes as indicated by the arrows in control littermates. TG mice expressed both WT- and MT-DLX3 proteins in the nucleus of osteoblasts (arrow heads) and osteocytes (arrows). Higher magnification shows localization of WT- and MT-DLX3 proteins in nucleus (inserted images). Pre-bleed serum was used as a negative control (Pre Ab). (E) Immunofluorescence double labeling demonstrating the WT-DLX3 (red) (c) and MT-DLX3 (b) proteins expressed in the nucleus of primary osteoblasts from TG mice (d; merge, a; phase contrast).

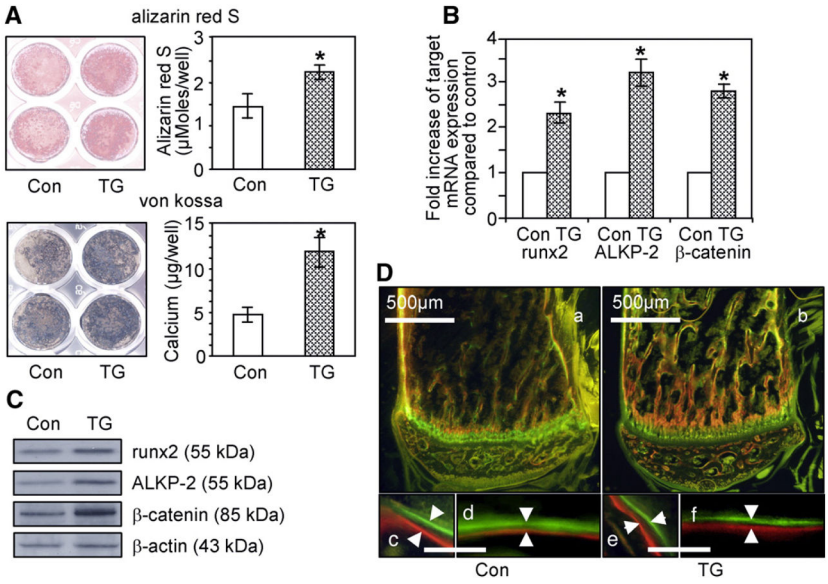

Fig. 4.

Effects of MT-DLX3 on osteoblastic bone formation in male mice. (A) Calcium deposition was detected with alizarin red S and von Kossa staining using bone marrow stromal cells from 6 week old mice. TG mice show enhanced alizarin red S and von Kossa staining (left panels). Quantification of alizarin red S and calcium revealed more nodule formation in TG mice (right panels) (*p*: * <0.05, data represent mean±SEM). (B) mRNA expression levels by real time PCR for runx2, ALKP-2, and β-catenin. Fold increase represent the ratio of 2^-(Ct(Target)-Ct(GAPDH))$^{(TG)}$ versus 2^-(Ct(Target)-Ct(GAPDH))$^{(Con)}$ (*p*:* <0.05, data represent mean±SEM). (C) Protein expression levels of runx2, ALKP-2, and β-catenin in primary osteoblasts by western blot analyses. (D) TG mice did not show enhanced dynamic bone formation rates in *in vivo* fluorochrome double labeling experiments using alizarin red S and calcein, as indicated by white arrows (a,c,d, control; b,e,f, TG mice; a,b, low power; c,d,e,f, high power; c,e, trabecular bone; d,f, cortical bone; lower bar=10 μm).

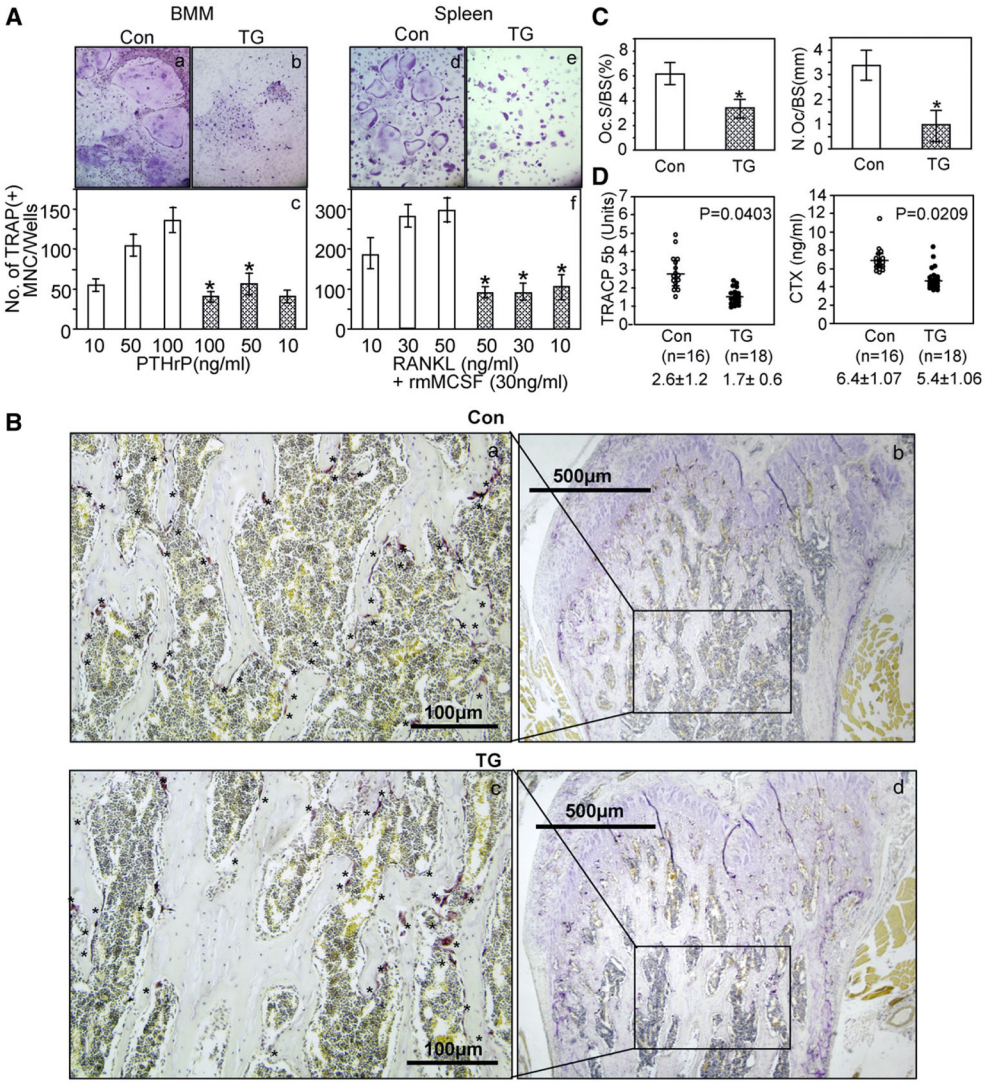

Fig. 5.

Effects of MT-DLX3 on osteoclastic bone resorption in 6 week old male mice. (A) Bone marrow monocytes (BMM) (a,b) and spleen cells (d,e) were isolated from MT-DLX3 TG (b,e) and control littermates (a,d) and differentiated into osteoclasts using varying concentration of osteoclastogenic factors. The numbers of TRAP(+) MNC stimulated by PTHrP were not increased in cultured bone marrow cells from MT-DLX3 mice (hatched bar) compared to those of control littermates (open bar) (c). Similarly, the numbers of TRAP(+) MNC stimulated by rmMCS-F and RANKL were not increased in cultured spleen cells from TG mice (hatched bar) (f) (*p*: * <0.05, data represent means±SEM). (B) TRAP staining was performed on femora bone sections. TRAP(+) osteoclasts (OCL) are indicated (with * on the surface of trabecular bone in the distal metaphyseal area of femora from control littermates (a,b) and TG mice (c,d)). (C) Histomorphometric analysis of osteoclast surface per bone surface [Oc.S/BS (%)] (left panel) and the number of osteoclast per bone surface [N.Oc/BS(mm)] (right panel) were performed in three consecutive slides from control littermates (open bar) and TG mice (hatched bar) (*p*: * <0.05, data represent means

±SEM). (D) Serum levels of TRACP 5b (left panel) and CTX (right panel) were significantly decreased in TG mice.

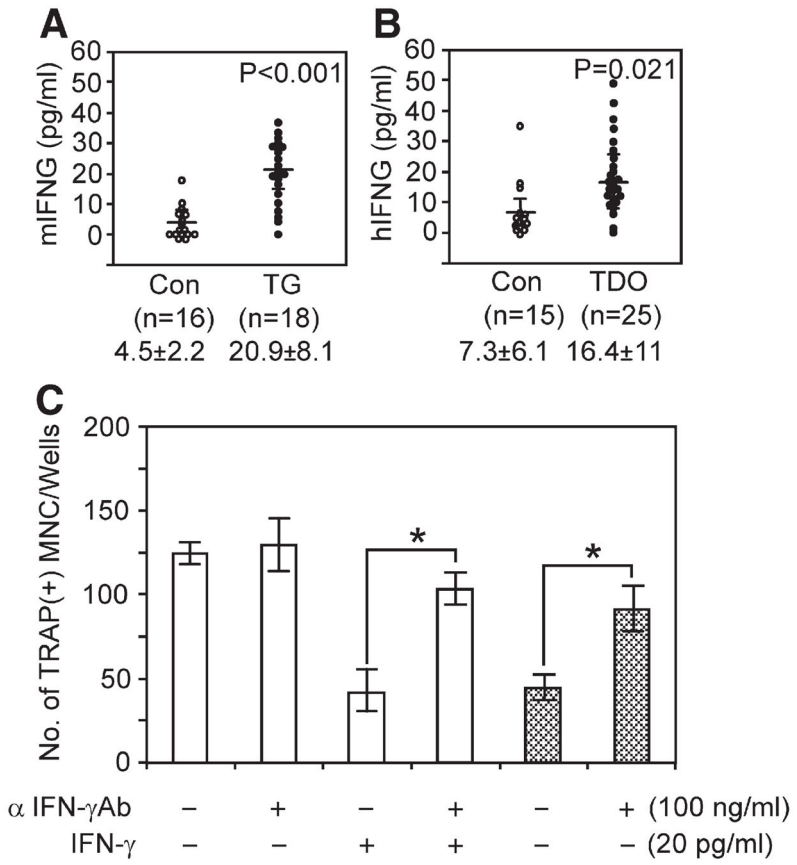

Fig. 6.

Expression levels of IFN-γ and effect of IFN-γ on osteoclast formation. (A) Expression levels of mouse IFN-γ measured by ELISA kit using mouse serum from TG mice and control littermates. (B) Expression levels of human IFN-γ measured using serum specimen from patients with TDO syndrome (*n*=25) and unaffected sibling (*n*=15). (C) Effect of anti mouse IFN-γ antibody on osteoclast formation. Mouse bone marrow cells from control littermate (open bar) and TG mice (hatched bar) were stimulated with 30 ng/ml of RANKL in the presence and absence of 100 ng/ml of anti mouse IFN-γ antibody and 20 pg/ml of IFN-γ. (*p*: *<0.05, data represent means±SEM).